Small bubbles formation and contribution to the overall gas holdup in large diameter columns of very high viscosity oil

Shara K. Mohammed [a,b,*], Abbas H. Hasan [c], Georgios Dimitrakis [a], Barry J. Azzopardi [a]

[a] *Department of Chemical and Environmental Engineering, Faculty of Engineering, University of Nottingham, Nottingham, UK*
[b] *Department of Petroleum Technology, Erbil Technology College, Erbil Polytechnic University, Erbil, Kurdistan Region, Iraq*
[c] *Department of Chemical Engineering, Faculty of Science and Engineering, University of Hull, Hull, UK*

ABSTRACT

A limited number of studies are available in literature on the small bubbles which create from gas-very high viscosity oils interaction and its contribution to the gas holdup in the system. The rate of small bubble formation has an important impact on heat and mass transfer in many chemical and industrial processes. The work presented in the current paper provides unique information on the formation of bubbles of millimetre diameter in high viscosity oil. A column of 290 mm diameter and Silicon oil of 330 Pa.s viscosity, were employed besides Electrical Capacitance Tomography and a high-resolution camera to investigate the characteristics of the small bubbles. Mechanism of bubble generation, effect of gas injection time and flowrate were studied. The average void fraction, total gas-liquid height, overall Probability Density Function (PDF) profile, small bubbles volume fractions and diameter were measured. Small bubbles generate from the eruption of large bubbles, at gas injection nozzles, coalescence of large bubbles, and at liquid bridges at transition to churn flow regime. Properties and concentration of the small bubbles are controlled by the location of the bubble generation, gas flowrate, and gas injection time. Small bubbles contribute by 6.6- 30% to the total gas holdup. Bubble diameter increased from 0.68 mm to 0.75 mm and decreased from 1.1 mm to 0.75 mm at the top and the bottom sections of the column respectively after 60 minof gas injection.

1. Introduction

In two phase gas-liquid flow systems, small bubbles of millimetres are created due to the interaction between the gas and the liquid. These bubbles accumulate in the system due to the slow motion and the ineffective mixing of the fluids as a reason of the high viscosity mediums. Small bubbles holdup in viscous liquids has a numerous importance in chemical and industrial processing. The hydrodynamics of the small bubbles have a significant effect on the heat and mass transfer processes often employed in the petrochemical, biochemical, refining operations, and polymer industries. A significant number of studies has been focused on the gas holdup and the physical properties of the small bubbles in water and low viscosity liquids, (de Jesus et al., 2017; Jamshidi and Mostoufi, 2017; Ding et al., 2019; Lucas and Ziegenhein, 2019; Kováts et al., 2020; Liu, 2020; Maldonado, 2020).

The majority of the studies on small bubble beds were conducted by using water or other low viscosity liquids (Shah, 1982; Lubbert, 1988). However, a smaller number of studies used viscous liquids with

viscosities of approximately t 1 Pa.s, (Shah, 1982; Schumpe and Deckwer, 1987; Philip, 1990; Kawalec-Pietrenko, 1992; Kastánek et al., 1993). Small bubbles are created from the eruption of large bubbles at the top surface of the liquid. The curved film which retracts from the ruptured bubbles, traps air forming an unstable toroidal geometry. Therefore, a ring of small bubbles is created at the top section of the liquid. The mechanism of the small bubble generation (daughter bubble) was studied by Bird (2010) using two synchronised high-speed cameras. The first camera was placed at the side and second was placed below the bubbles. Fig. 1 displays the two stages of small bubbles' creation from the eruption of larger bubbles in 0.31 Pa.s viscosity glycerol-water. First is the collapse of the liquid film above the large bubble and the trapping of the air after falling down. The second stage is the forming of the small bubbles after the breakup of each torus of trapped air. The creation of the small bubbles in viscous liquids (1.5 Pa.s castor oil) was studied earlier by Pandit (1987). They proposed two mechanisms for generating small bubbles of 0.5-2 mm diameter. One relating to the eruption of large bubbles of 10-50 mm diameter, and another one relating to the gas

injection points.

The first mechanism, which relates to the eruption of the large bubble, is the same as the one proposed later by Bird (2010). The second mechanism for the creation of the small bubbles relates to the coalescence and the break-up of the large bubbles at the gas nozzles. According to Otake (1977) and Pandit (1987), the small bubbles are generated from the tail which is created during the coalescence of the bubbles at the gas inlet point. This tail breaks up to smaller bubbles after it gets elongated. Then the small bubbles are carried up by the liquid motion. A similar mechanism for the generation of small bubbles was shown by Pioli (2012) and Azzopardi et al. (2014). Bird (2010) reported that the amount of the trapped gas which is produced from the eruption of the large bubble is controlled by a number of factors; (a) the capability of the collapsed liquid film to bend inward at the top surface of the liquid, (b) the stability of the area surrounding the large bubble at the top surface, (c) the amount of the energy which is required for the large bubble to rupture. Therefore, increasing the pressure inside the large bubbles increases the curvature of the film and produces more small (daughter) bubbles.

The small bubbles, which are generated in high viscosity liquids, accumulate in the system due to their low rising velocity. At low gas flow rates, the liquid slugs rise at low velocity and carry the small bubbles. The rise velocity of the small bubbles increases with increasing the gas flow rate due to increasing the rise velocity of the large bubbles which in turn push the liquid slug upward. This circulation motion of the liquid enhances the mixing and the releasing of the small bubbles. Philip (1990) studied the gas holdup, bubbles rise velocity and the liquid circulation in 0.15 m diameter column using liquids viscosities range of 1-3 Pa.s. They noticed small bubbles of <1 mm diameter, which may contribute to about 50% of the gas holdup. These small bubbles are seen to accumulate in the pipe due to their low rising velocity. Less than 1% of the injected gas to the system appeared to convert into small bubbles in high viscosity liquids. These small bubbles are generated due to the coalescence of the large bubbles at the gas injection points and due to the bubble eruption at the top surface of the column. The void fraction, due to small bubbles in slug flow, increases with an increasing liquid viscosity which in turn decreases the velocity of the slug units. This low velocity of the liquid produces less circulation for the liquid in the column due to low rise velocity of the liquid slugs. The void fraction (the small bubble concentration) increases also with increasing the time of the gas injection and the gas flow rate. Philip (1990) also found that a time of 15-60 min is needed to achieve stable void fraction values due to increasing the concentration of the small bubbles. However, Kuncová and Zahradník (1995), who employed liquids with viscosities of 1-30 m Pa.s over a wide range of gas flow rates, showed quite different results. They found that the concentration and the void fraction of the small bubbles are independent of the time of gas injection at low and intermediate gas flow rates.

However, a different conclusion was reported for the void fraction of the small bubbles in gas-viscous liquids flow by Kuncová and Zahradník (1995). They stated that the small bubbles holdup increases with increasing liquid viscosity, while it decreases with an increasing gas flow rate. Similar studies in the literature focused on the behaviour of the small bubbles in gas-liquid flow by Azzopardi and Zaidi (2000), Schäfer et al. (2002), Mena (2005), Majumder et al. (2006), Bröder and Sommerfeld (2007).

A considerable research on the size distribution of the small bubbles was carried out by using digital image methods. Lau (2013) and Aoyama (2016) studied the small bubble size distribution, gas holdup and the shapes of the single bubbles rising in stagnant liquids of different viscosities. In both studies, a method by Otsu (1980) was used for the small bubbles image processing. The small bubble size distributions were also studied by Lage and Espósito (1999), Wongsuchoto et al. (2003), Mandal et al. (2005), Bordel et al. (2006), Montante et al. (2008).

In all the afore mentioned the studies reported, it appears to be a distinctive lack of information regarding the formation of small bubbles trapped in a very high viscosity liquids and large diameter columns. The present study attempts to address this gap by providing additional information on the formation of small bubbles in such systems. The main aim of the present is to provide new information on the dynamics of creation and the characteristics of small bubbles (millimetres to centimetres) which accumulate and flow in a column of gas-very high viscosity oils. A column of 290 mm diameter, Silicon oil of 330 Pa.s viscosity, and 3.60 m liquid initial height were used in this study. A high-resolution camera was employed to investigate the creation of the small bubbles at different locations on the column. Electrical Capacitance Tomography (ECT) was used for the total gas holdup measurement in the column. The mechanism of the bubble generation, effect of gas injection time, the contribution of the small bubbles in overall void fraction, and the characteristics of the bubbles in gas-viscous oil flow were studied. Gas holdup/average void fraction, small bubbles volume fractions at different locations were measured. Bubble dimension and the Probability density Function (PDF) of the small bubbles diameter were also determined at different locations and times of gas injection.

2. Experimental setup

A set of experiments was carried out to study the dynamics of, centimetre to millimetre in diameter, bubbles' creation in high viscosity oils. The experiments carried out in the faculty of engineering laboratories at the University of Nottingham. Silicone oil of 330 Pa.s viscosity, surface tension of 0.02 N/m, density of 950 Kg/m^3 was used with compressed air in 290 mm diameter column. The initial hight of the oil
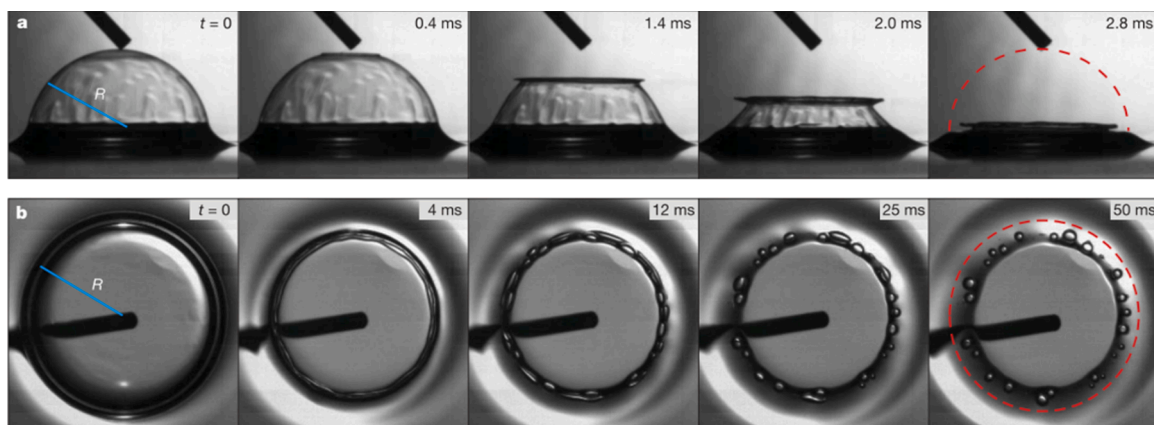

Figure 1. High-speed images showing the mechanism of the small bubbles creation at the top section of the glycerol-water mixture with a viscosity of 0.31 Pa.s is from the side and b is from below (Bird, 2010).

in the column was 3.36 m. The column was provided with 25 gas injection nozzles of 4 mm diameters which distributed equally at the bottom of the column. Groups of 5 nozzles were connected with a flow regulator to allow a full control of the number of the nozzles used in the experiments. Moreover, two types of flowmeters with two different flow ranges were used, very low-very high capacity (5-5000 L/m), to achieve a wide range of gas flowrate. The dimensions of the experimental rig are illustrated in Fig. 2.

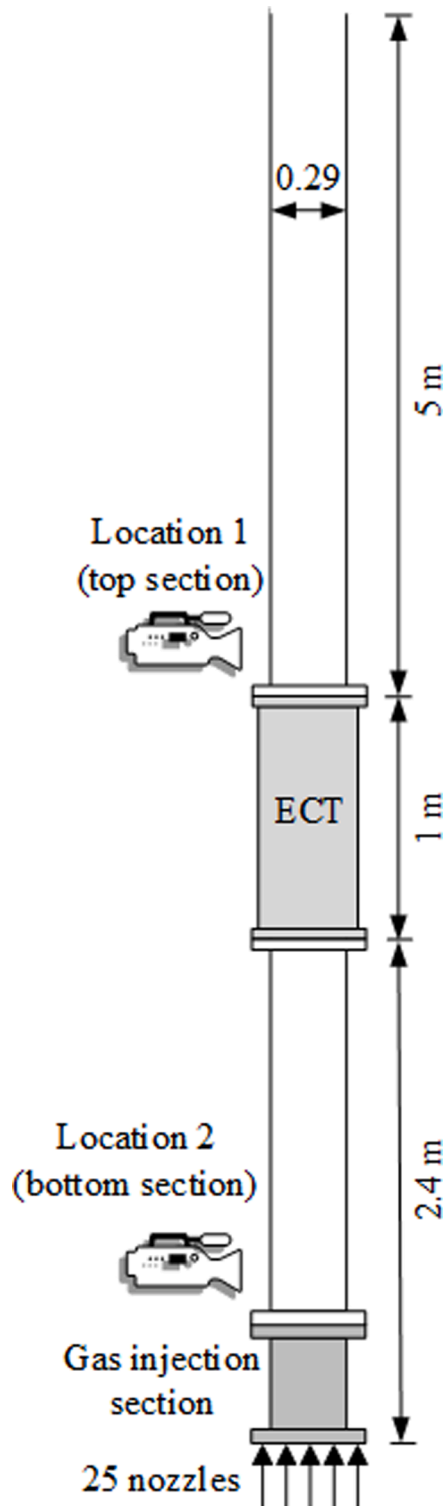Two experimental settings were conducted using two different

Figure 2. Experimental setup

measurements techniques. First, Electrical Capacitance Tomography (ECT) to examine the contribution of the small bubbles in the overall gas holdup in the column by controlling the time and the volume of the gas injection. In this work, the "time of gas injection" refers to the period of time (duration) which the gas was injected into the column continuously. Gas was injected for 6 h and measurements were obtained every 30 min using ECT which is located at 2.4 m from the gas inlet section, see Fig. 2. Gas was injected at three different gas superficial velocities, 0.01, 0.047, and 0.178 m/s corresponding to bubbly, slug and slug-churn transition flow regimes respectively. To achieve this wide range of gas superficial velocities, 25 gas nozzles were used in this experiment. Fig. 3 shows the configuration of the gas nozzles at the bottom of the column. The gas injection points are distributed equally at the gas inlet section. The capacitance non-intrusive technique measures the cross-sectional distribution which can be correlated to measure the mean phase distribution in the column. The ECT was validated by Montante et al. (2008), Azzopardi (2010), and Pradeep (2014) and calibration procedure was explained by Mohammed (2018). In addition, more detailed information was reported by Abdulkareem (2011). The time averaged void fraction was calculated from the time series data which obtained from the ECT. Void fraction or gas fraction is a dimensionless value (between 0 and 1) that represents the cross-sectional area occupied by the gas in two phase gas-liquid flow (Bertola, 2003). The liquid holdup/liquid fraction, ε_l which was measured using the ECT was used to calculate the Void fraction, ε_g, $\varepsilon_g + \varepsilon_l = 1$. The void fraction in combination with the PDF was used to identify the overall structure of the flow. The PDF profile is a common method used for flow structure identification (Costigan and Whalley, 1997). It was calculated from the variation of the amplitude frequencies of the time series of void fraction using the histogram method.

In the second set of experiments, a high-resolution camera, Canon EOS 600D, 18-megapixel resolution was used with LED panel light PS0606-6W which was installed behind the column. Horizontal and vertical resolutions of 72 dpi were obtained for the photos which were taken by the camera. The camera was placed in two locations, at the top section of the liquid and at 0.6 m from the gas injection points, see Fig. 2. The measured positions of the small bubbles were close to the column wall, as the diameter of the column is very large compared with the diameters of the bubbles. Therefore, the curvature of the wall was neglected as the distortion is very small.

In this set of experiments gas was injected at a gas superficial velocity of 0.006 m/s through 5 nozzles for one hour. The reason of using 5 gas nozzles was both technical and operational. Five nozzles are the maximum number that could be used to achieve 0.006 m/s gas superficial velocity using a low-pressure gas line. The chosen nozzle configuration had one at the centre and 4 nozzles distributed equally next to the pipe wall at the gas inlet section as shown in Fig. 4. The circumferential distance between the nozzles next to the pipe wall is 164.9 mm. The radial distance between the nozzle at the centre and the 4 nozzles is equal to 105 mm. Photos were taken at the top and bottom sections (about 60 mm from the bottom of the column) of a 290 mm diameter column. Photos were captured after 10 and 60 min of gas injection. The gas injection was stopped during every photo shoot. The reason behind that was to obtain a homogenous (presentable) unit volume of small bubbles for gas hold up measurements. In another words small bubble distribution vary significantly during gas flow (large bubbles flow) throughout the column. This is in addition to the difficulty of capturing clear photos for image analysis of the small bubbles in the presence of the large bubbles.

In the bubble concentration analysis, photos of the oil in the column were taken (in the absence of the bubbles) to obtain the background which will be used as a threshold. The RGB photos of the bubbles were inverted to greyscale images. Then they were converted to a binary image by using the threshold, applying the method by Otsu (1980). Using a MATLAB® code, the small bubbles were selected by specifying the number of objects. It labels each object (bubble) in the image with an
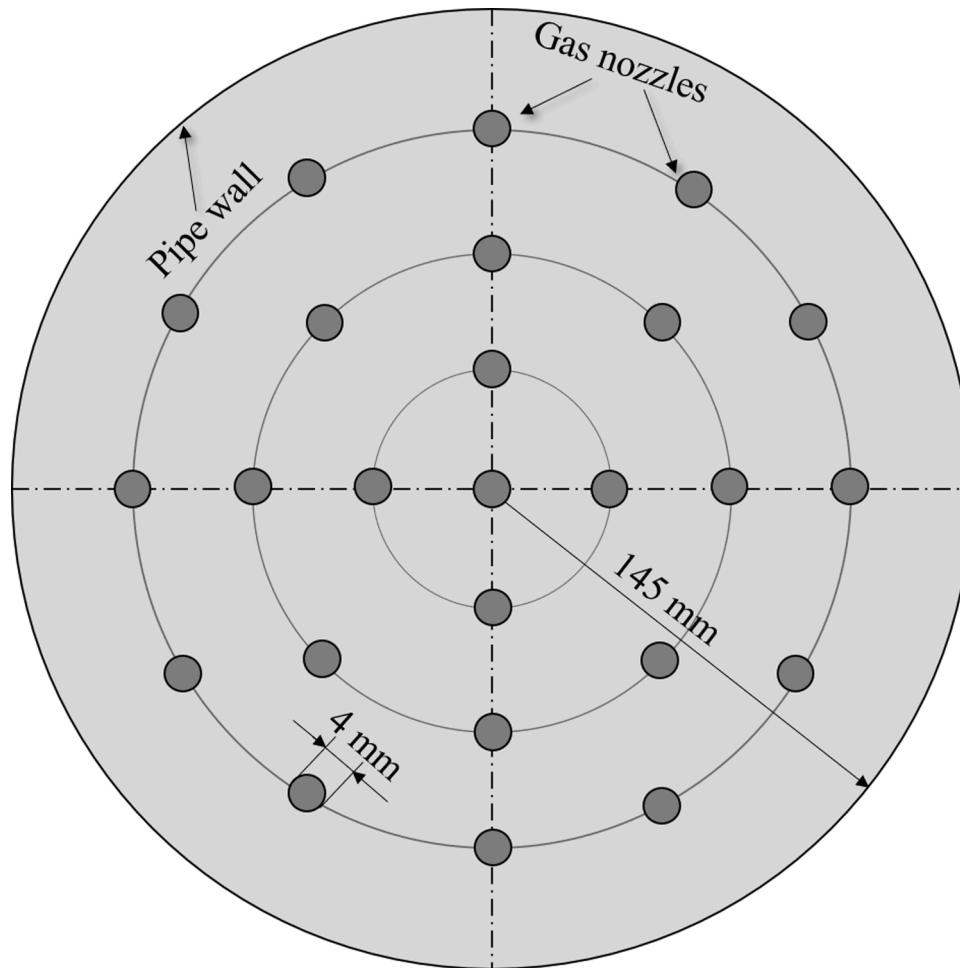
Figure 3. A schematic drawing for the gas inlet section at the bottom of the column showing the 25 gas nozzles of 4 mm diameter.

integer value. Then the area was converted to volume by multiplying by the thickness (depth) of the tested area. The thickness was selected from the average diameter of the small bubbles. The percentage of the determined volume of the small bubbles was calculated by dividing the volume of the bubbles by the total volume of the image.

Second, the diameters of the small bubbles were determined using the ImageJ software. This software enables to define the bubble boundary and calculate the area, circumference, minor axis, major axis, and the diameter of the selected objects. The images were calibrated by using a measuring tape placed on the column for scaling purpose. The diameters of about 95-57 bubbles, at the top and the bottom of the column respectively, were determined to calculate the average diameters of the small bubbles at each time.

3. Results and discussion

Small bubbles, in this work, refer to bubbles of millimetres to centimetres diameter which create from the interaction between gas and very high viscosity oil. In viscous mediums, the small bubbles accumulate in the system due to their low rising velocity (Philip, 1990). The main sources of these bubbles are from: the rupture of large bubbles at the top surface of the liquid, the gas injection points section, and from the coalescence of the large bubbles, (Pandit, 1987). The gas-liquid interaction structure in systems of very high viscosity oils shows different behaviour in compare with water and low viscosity liquids (Hasan, 2019; Mohammed, 2019). This work focuses on the dynamics of the small bubble generation in 330 Pa.s oil at different locations and flow regimes. The "large bubbles" refer to spherical bubbles of diameter

approximately equal to 2/3 pipe diameter appear at bubby and slug flow. Two classifications can be applied to categorise the small bubbles. The first is the bubbles size since two main scales of the bubbles were observed (millimetres and centimetres). The second, is the source of the bubble's generation, as they were created from three main sources. In the present study, the focus will be on the second classification to study the small bubbles in high viscosity liquids.

3.1. Visual observation

According to the visual observation, the small bubbles were generated from three main locations in the column. The size, the shape and the population of the small bubbles were mainly controlled by the location of the bubble generation. The structure of the flow also played a considerable role in the creation of this type of bubbles. For example, the main source of the small bubbles was different in bubbly and slug flow than the transition to churn flow. In the bubbly and slug flow regimes, the main source was the burst of the bubbles at the top surface of the liquid. While at the transition to churn flow regime it was seen at the churn regions due to the high interaction activity between the two phases. Therefore, small bubbles in high viscosity liquids generate from: bubble eruption at the top surface, gas injection points at the bottom of the column, coalescences between the large bubbles, and finally the churn regions in the column at high gas flowrates.

3.1.1. Top section (bubbles eruption)
At bubbly and slug flow regimes, the large bubbles rise in the column due to the balance between the buoyancy and drag force. The large
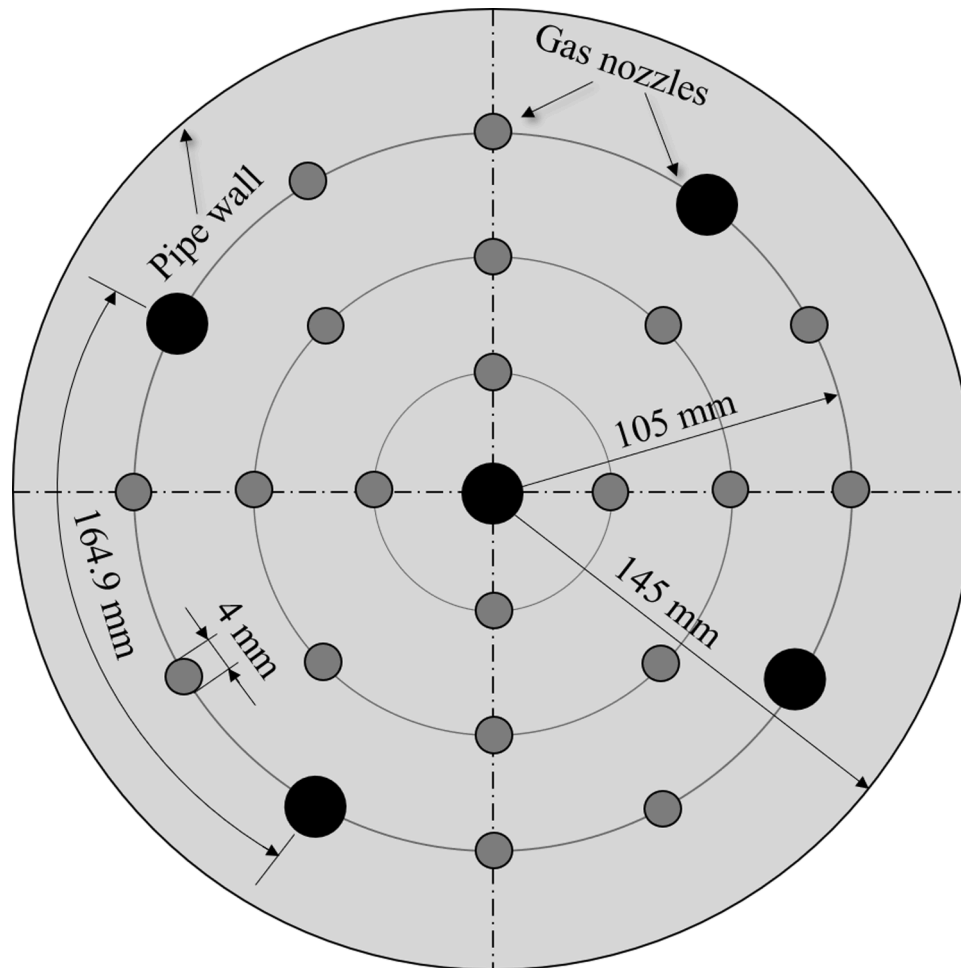
Figure 4. A schematic drawing for the gas inlet section at the bottom of the column showing the 25 gas nozzles of 4 mm diameter. The black bold points correspond to the 5 gas nozzles used to achieve a 0.006 m/s gas superficial velocity in the second set of experiments.

bubbles push the liquid slugs at the top of the bubbles until a very thin film remains at the top of the bubble (1 and 2 in Fig. 5). Then the thin film collapses (bubble burst, (3)) and falls on the top surface of the liquid (4 and 5), while the next liquid slug still pushing the bottom of the erupted bubble, 6 in Fig. 5. In bubbly flow, when the diameter of the large bubbles is smaller, the collapsed film falls on two positions, the liquid ring around the erupted bubble and inside the erupted bubble (the bottom of the bubble). While at slug flow regime, when the bubble diameters are closely or approximately equal to the column diameter, the film remains on the pipe wall and drains to merge with the liquid. The film, which results from the bubble eruption in both cases, traps air and creates a ring of unstable bubbles. These temporary bubbles, in turn, create smaller bubbles due to the shearing by the liquid motion on the pipe wall in case of higher gas flow rates. The amount of the small bubbles, which are generated in higher gas flow rates, is higher not only because of increasing the surface area of the liquid film but also due to increasing the frequency of the bubble eruption. The mechanism of small bubble generation at the top surface of the liquid was studied by Pandit (1987), Seyfried and Freundt (2000), Bird (2010), Hasan (2019). The small bubbles, which are created at the top surface, are smaller in diameter, relatively equal in size, homogenous, higher in concentration compared with the other small bubbles from different sources and locations in the column. They spread inside the column by the circulation motion of the liquid due to the rising of the large bubbles, which push a fraction of the liquid down as a falling film.

3.1.2. Gas inlet section

The small bubbles were also seen to be generated from the gas inlet section at the bottom of the column. The bubbles generated from this this area appeared to have different characteristics to the ones generated at the top section. They were not homogenous, as the variation in bubbles size is very large due to the mechanism of the bubble generation at this area. Fig. 6 shows a picture of the small bubbles at about 0.6 m from the gas inlet point. In this figure, only one gas nozzle is employed to inject the air with two different positions and equal gas flow rates, one at the centre of the column and another at 105 mm from the centre (next to the pipe wall). In general, the small bubbles are created from the rapid break up or coalescence of the large bubbles at the gas nozzles. The large drag forces are increasing the possibility of the coalescence at the gas inlet points. However, the effect of the shearing at the pipe wall can be clearly seen in the figure, when the nozzle next to the pipe wall is used. The rate of the breaking up of the large bubbles increases due to the friction by the wall. The rate of the small bubble creation is higher, the shape and the size of the bubbles are not structured. Since 25 gas injection points were used in this work at high gas flow rates, the possibility of the interaction between both fluids increases at this position. Therefore, more friction, more coalescence and more breaking up of the large bubbles occur at the gas inlet section due to creating one single bubble, at a time, from 25 gas nozzles. The mechanism of the small bubble generation at the gas inlet section was produced by Pandit (1987) and Philip (1990). The effect of gas injection methods, including increasing the number of the gas nozzles in 360 Pa.s Silicon oil and 240 mm diameter column is investigated by Mohammed (2021). In general,
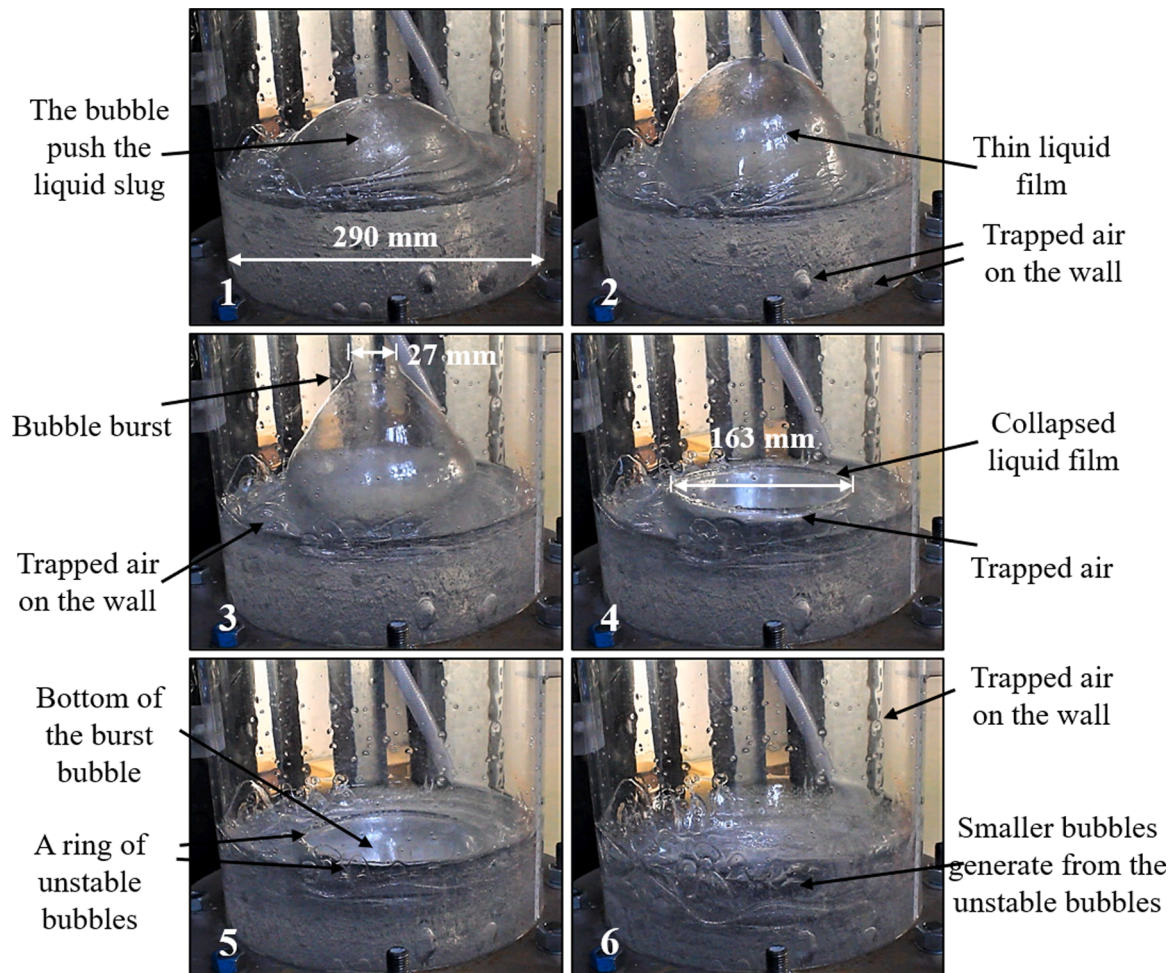
Figure 5. The large bubbles eruption at the top surface of a column of 330 Pa.s Silicone oil. The dimensions in the photos 3-4 correspond to the diameter of the hole created from the ruptured film. Total time from 1-6 is 7 seconds.

a number of temporary ellipsoidal bubbles with a length that varies from 4 cm to 1 cm and diameter from 2 cm to 2 mm were seen in this section. These small bubbles either rise with the liquid slug then coalesce with other bubbles or remain on the pipe wall and shear to create smaller bubbles.

3.1.3. Liquid bridges (Transition to churn flow)

The small bubbles which produced at churning regions/liquid bridges are relatively different due to the complicated structure in the transition to churn flow regime besides the very high gas flow rate. Factors such as the high frequency and the unstable direction of the motion of the liquid bridges in addition to the high interaction between both fluids and the drainage of the liquid film play role in the generation of the small bubbles. Details about the structure of churn flow in high viscosity liquids are presented by Mohammed (2018). The small bubbles, in this case, are not uniform in size and shape. However, the rate of increasing the concentration and the distribution of the small bubbles is very high due to the high gas flowrate and the motion of the liquid. Fig. 7 shows the structure of the transition to churn flow (0.178 m/s gas superficial velocity) in 330 Pa.s Silicone oil. The liquid bridges, which are the main source of the small bubbles as a reason of the high interaction activity between the two phases, appear to dominate the flow structure.

3.1.4. Bubble coalescence

Another source for the small bubbles generation is the coalescence between pairs of large bubbles when rising in the column, see Fig. 8 in Section 3.2. The small bubbles are produced mainly due to the entrainment of two large bubbles of different rising velocity. This phenomenon was studied by Philip (1990), Manga and Stone (1994). Small bubbles also seen to produce due to the effect of the large bubble wake when the bottom of the upper bubble changes from rounded into concave. When the two large bubbles merge, the liquid at the bottom of the lower bubble remains as a thin liquid film until it collapses at the last stage of the bubble coalescence. This liquid film also generates small bubbles, (Bhaga and Weber, 1981) and (Colella, 1999).

3.2. Overall gas holdup

In order to investigate the contribution of small bubbles in the overall gas holdup/time averaged void fraction in gas-high viscosity oils flow, gas was injected using five nozzles with constant flowrate into the column for 6 h and collecting data every 30 min. Three different gas superficial velocities, 0.01, 0.047, and 0.178 m/s, were applied in order to investigate the effect of the increasing gas flow rate. These gas superficial velocities were chosen to correspond to different flow patterns, bubbly, slug, and transition to churn flow, respectively. Time average void fraction and liquid height in the column were measured and compared in the column.

According to the visual observation, the amount of the small bubbles in the column increased significantly with the time of gas injection, even at a constant gas flow rate. Fig. 8 shows three photos of the column captured at the beginning (time: 10 min/ 0 h), middle (after 3 h) and at the end of the gas injection (after 6 h). The reason of referring to the 0 hr by 10 min is that each run/data acquisition time is 10 min. Therefore,
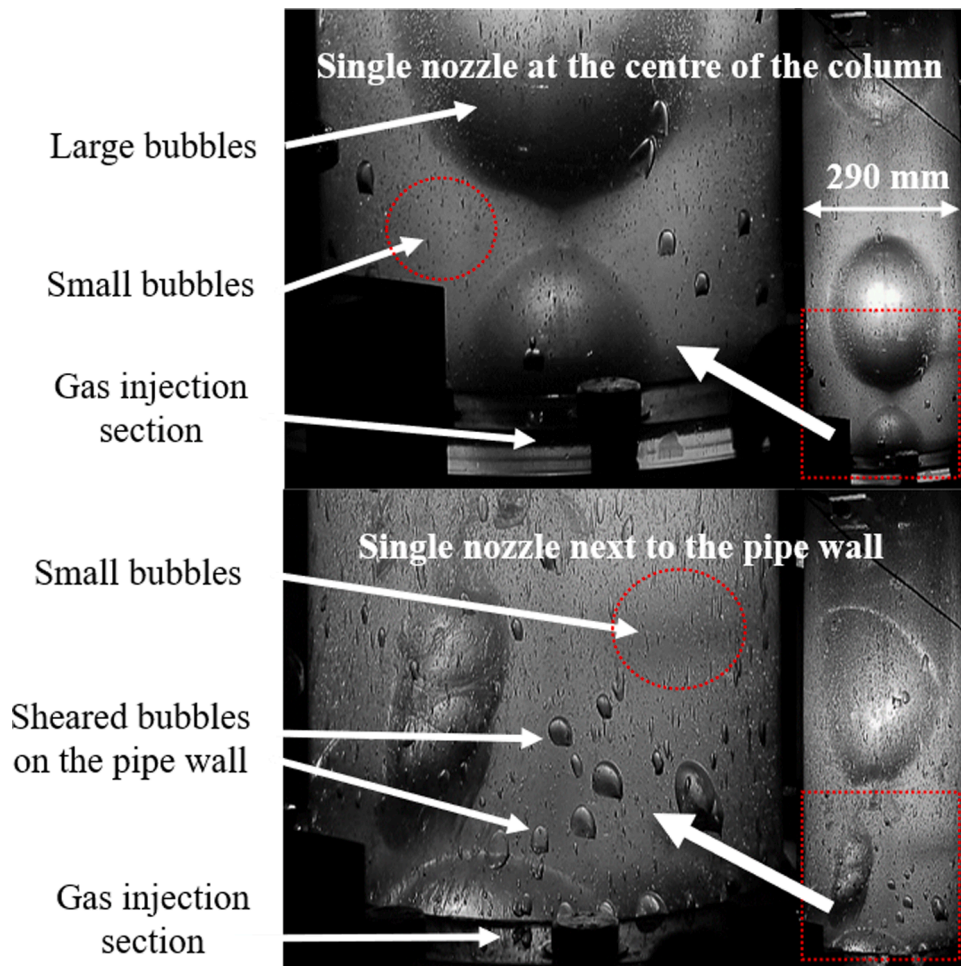
Figure 6. Generation of the small bubbles at the gas inlet section using single gas injection point with two different locations at a gas superficial velocity of 0.03 m/s (bubbly flow regime).

data at time 0 is actually an average of 10 min of data (30000 sample every 30 min). As the gas injection time proceeds, some bubbles, which hardly be released, sticks on the pipe wall. The shape, size, and rate of increasing of the small bubbles at this area do not depend only on the number and location of the gas injection points, but also on the time of gas injection.

The PDF, which is the variation of the amplitude frequencies of void fraction, was determined by using the histogram method. The frequency of the void fractions of the large bubbles and the small bubbles in the liquid slugs was also determined. Fig. 9 shows the PDF profile for bubbly flow (0.01 m/s gas superficial velocity) at the start, middle and end of the gas injection (6 h of continuous gas injection using 25 gas nozzles). The PDFs in Fig. 9 correspond to the photos in Fig. 8. The peaks with lower void fraction represent the void fraction in the liquid slug which contain the small bubbles. While the peaks of higher void fraction values are the void fraction of the large bubbles showed in Fig. 8. The void fraction from the small bubbles in the liquid slug increased significantly in the first (3 h) of the gas injection. Then, it increased slightly in the seconds 3 h. This could be related to the position of the ECT on the column which is located between the two main sources of the small bubbles (approximately middle of the gas-oil mixture). Therefore, at the start of gas injection the small bubbles generate from the large bubbles eruption at the top and the gas injection nozzles at the bottom of the column. Only a few number generate from large bubble coalescence as the rate of bubble coalescence is low at low gas flowrate (bubble flow), (Mohammed, 2019). In another words, the concentration of the small bubbles is lower at the middle of the column where the ECT is located.

Then, the small bubbles immigrate/disperse toward the middle from both ends of the column due to the mixing by the large bubbles. According to the PDF values, this process occurs at the first three hours in bubbly flow regime. This agrees with the photos in Fig. 8 which shows the small bubbles distributed nearly equally thought the column after three hours of gas injection. The contribution of the small bubbles in the overall void fraction increased with an increasing time of gas injection.

Fig. 10 shows the contribution of the small bubbles in the overall gas holdup in the mixture. It also compares the effect of increasing gas flowrate on the rate of the small bubbles generation. Overall void fraction increases by 0.02, 0.03, and 0.13 at gas superficial velocities of 0.01, 0.047, and 0.178 m/s, respectively. Therefore, the small bubbles' contribution to the overall void fraction is 8%, 6.6%, and 30% for gas superficial velocities of 0.01, 0.047, and 0.178 m/s, respectively after 6 h of gas injection. The void fraction due to the small bubbles is higher at the lower gas flowrate (bubbly flow) due to the high frequency of the large bubble. However, at slug flow (0.047m/s), the percentage is lower because of the high coalescence rate between the large bubble which in turn reduce the frequency. This indicates that the major source of small bubble is from the large bubbles bursting at the top section in bubbly and slug flow. On the other hand, the very high value at the transition to churn flow is due to the high interaction between both phases as liquid bridges, (Mohammed, 2018). Standard errors in Fig. 10 are calculated from the standard deviation and the square root of the number of the repeated values. Maximum standard errors are 0.12% 0.11%, 0.11% for gas superficial velocities of 0.01, 0.047, 0.178 m/s, respectively.

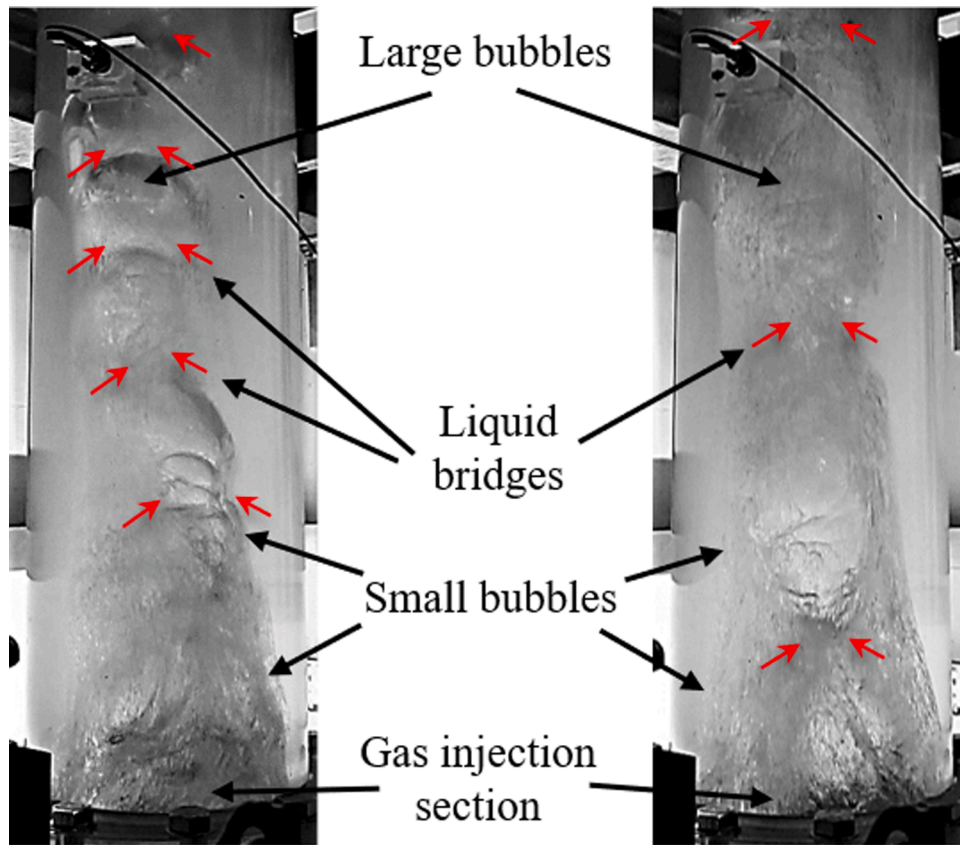Similarly, the total height of the gas-oil in the column appears to

Figure 7. Photos of the column showing the small bubbles formation at the liquid bridges (arrows in red) and at the gas inlet section, the gas superficial velocity is 0.178 m/s (transition to churn flow regime)
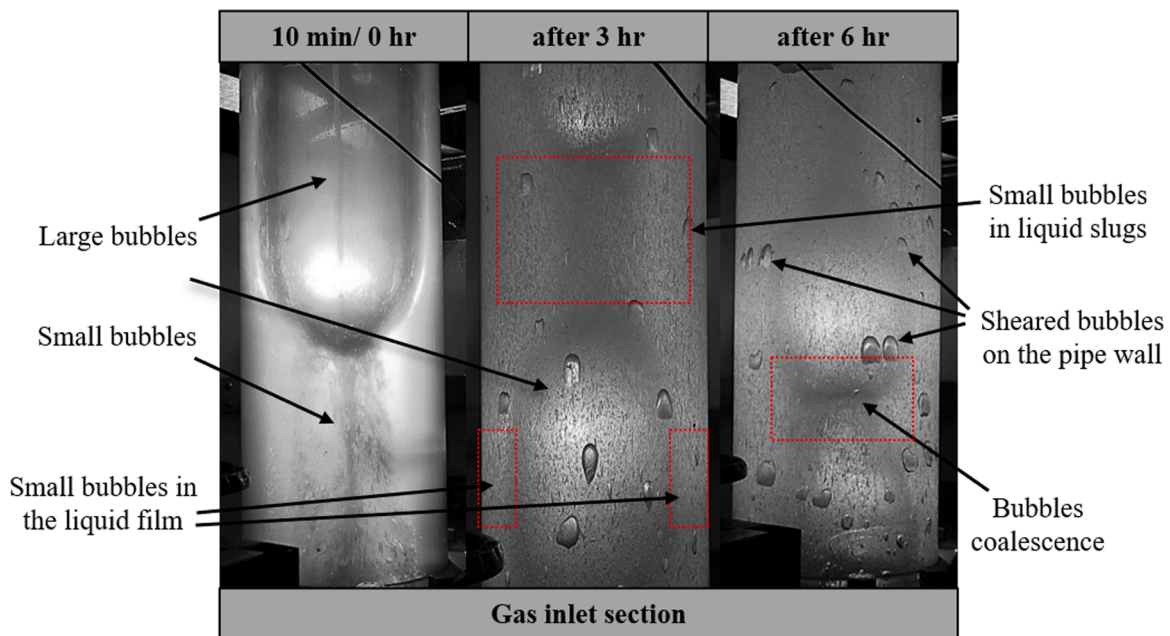

Figure 8. Photos of the 290mm diameter column at three different times showing the increase of the small bubbles concentration at a fixed gas superficial velocity (0.01 m/s)

increase slightly by injecting air using 25 nozzles for 6 h for all tested flow regimes. The initial height of the oil is 3.6 m (stagnant oil) and 4 m (at bubbly flow with gas superficial velocity of 0.01 m/s), 4.4 m (at slug flow, 0.047 m/s), and 4.3 m (at transition to churn, 0.178 m/s) at the start of gas injection. The height of the mixture increases steadily by 10 and 13.6 cm at gas superficial velocities of 0.01 and 0.047 m/s which correspond to bubbly and slug flow regimes, respectively. On the other hand, it seen to fluctuate at the transition to churn flow with a total
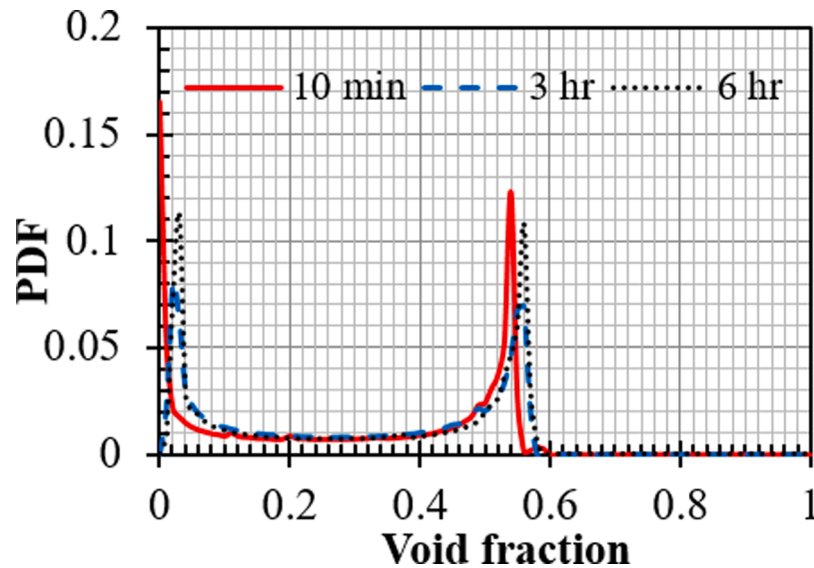
Figure 9. Probability Density Function profile for bubbly flow (0.01 m/s gas superficial velocity) in a column of 330 Pa.s Silicon oil and 290 mm diameter at three different time of gas injection. Total time of gas injection is 6 h..
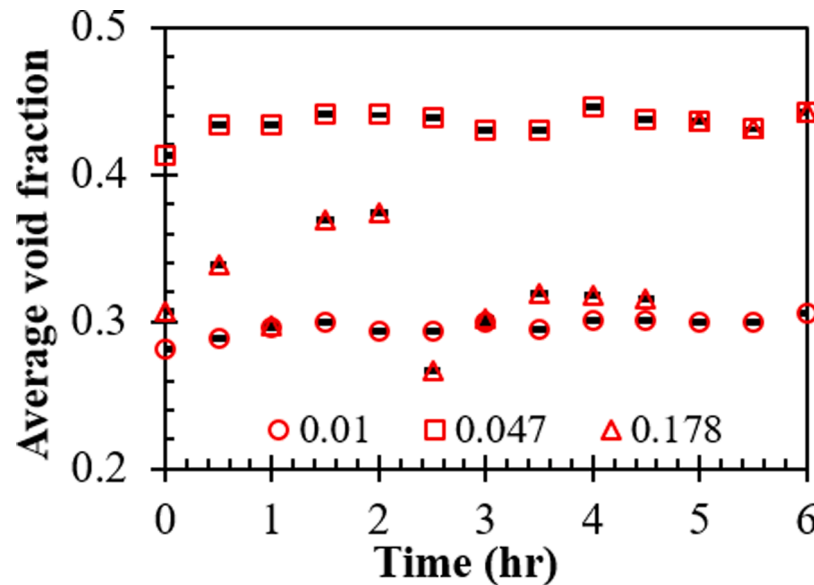

Figure 10. The contribution of the small bubbles in the time averaged void fraction (extracted from the ECT sensor) and the effect of time of gas injection on the time-averaged void fraction of gas flowing in stagnant 330 Pa.s Silicone oil in a 290 mm diameter column. Gas superficial velocities of 0.01, 0.047, and 0.178 m/s were applied using 25 gas nozzles.

increase of 22 cm in height, as shown in Fig. 11. This is due to the oscillations at the top surface of the oil which cause by the churning areas, detailed information about such churning features is reported by Mohammed (2018). Maximum standard errors which are calculated from the standard deviation and the square root of the number of the repeated values, are 0.1% 0.02%, 0.11% for gas superficial velocities of 0.01, 0.047, 0.178 m/s, respectively.

Comparing the total height of the gas-liquid mixture for bubbly and slug flows in the column shows an increase in the average height with increasing gas flow rate. This indicates increasing in the rate of the small trapped bubbles with increasing the gas flowrate. According to the visual observation the rate of increasing the concentration of the small bubble was much higher at high gas flow rates. This is due to the increasing frequency of the large bubble eruption and coalescence. Thus, the concentration of the small bubbles in the viscous liquid is not only proportional to the amount of the gas flow rate but also to the time

period of gas injection. This agrees with the results reported by Philip (1990).

3.3. Small bubbles concentration

The concentration of the small bubbles in high viscosity liquids is controlled by different parameters: gas flow rate, the location and the number of the gas injection points, column diameter, the viscosity of the liquid, and finally the time of gas injection. In this set of experiments, the rate of changing the concentration of the small bubbles in 330 Pa.s Silicone oil and 290 mm diameter column was determined at a constant gas flow rate. The gas was injected using 5 injection points at a gas superficial velocity of 0.006 m/s for 1 h. Photos of the column were taken after 10 and 60 min from gas injection at the top section of the liquid and the bottom of the column (0.6 m from the gas inlet). The gas injection was stopped when the photos were taken to obtain a clear image of the
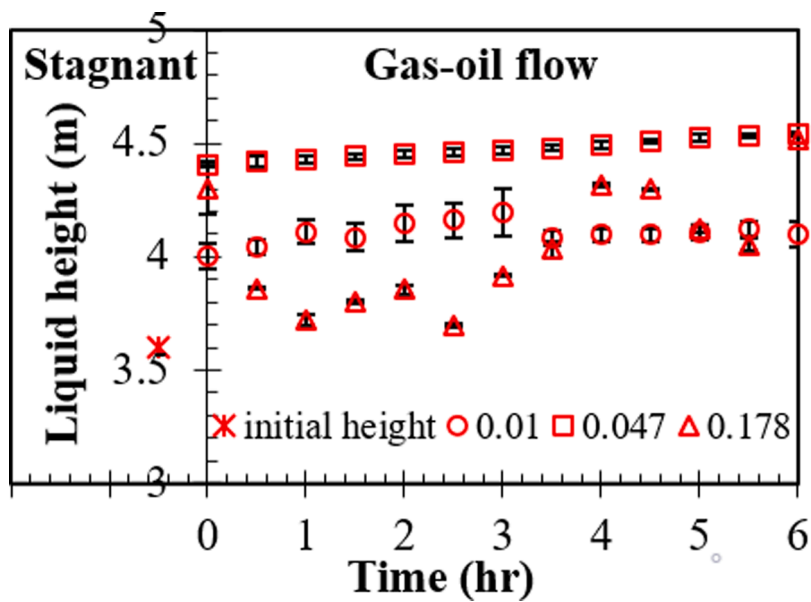
Figure 11. Height of the gas-liquid during 6 h of gas injection at three different gas superficial velocities corresponding to bubbly (0.01m/s), slug (0.047m/s) and slug-churn transition flows (0.178m/s).
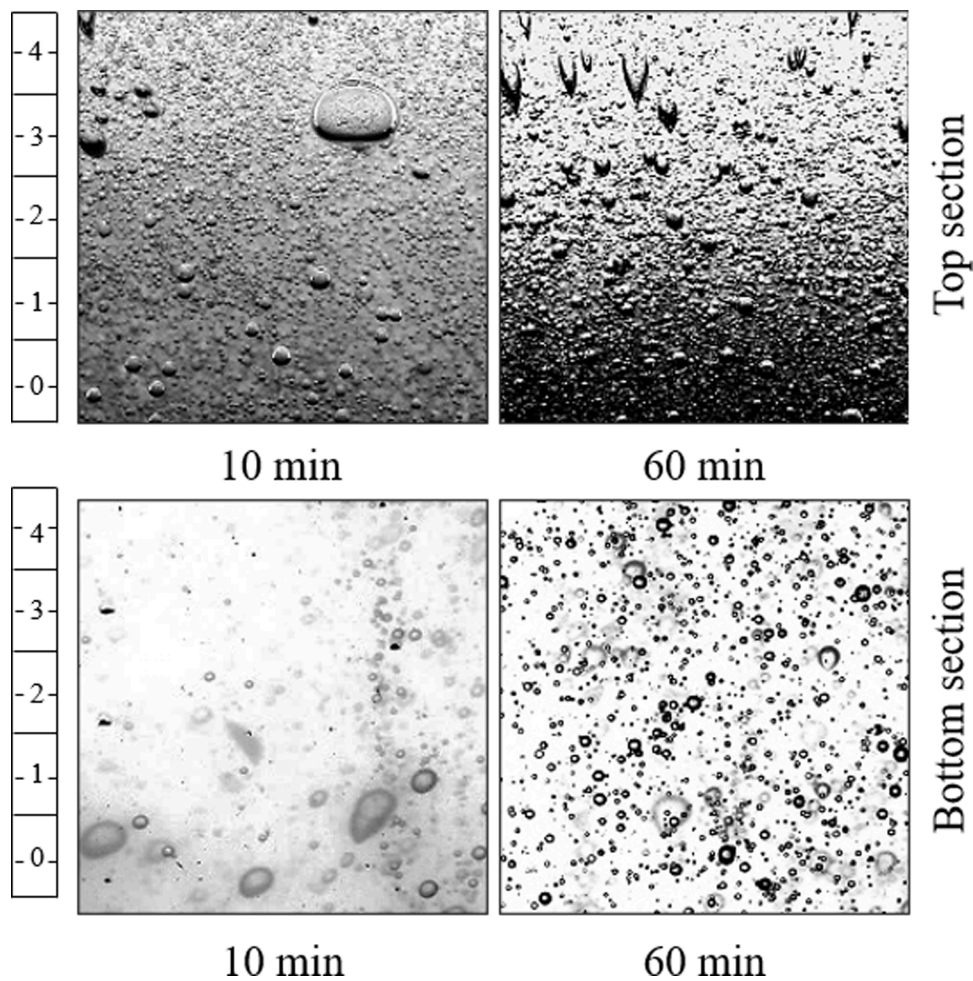

Figure 12. Small bubble creation in high viscosity liquid at the top and bottom sections of the column. Photos were taken after 10 and 60 min of gas injection at a gas superficial velocity of 0.006 m/s. The gas injection stopped when the photos were taken. The resolution of the images is 28.85 Pixel/mm and the scale in the photo is in centimetres.

small bubbles only and to avoid the effect of the large bubbles. Similar works in literature have been done to study the small bubbles behaviour in gas-liquid flow by Fraser et al. (1963), Azzopardi and Zaidi (2000), Schäfer et al. (2002), Mena (2005), Majumder et al. (2006), Bröder and Sommerfeld (2007). The difference between the previous works and the present work is that, in this work, a <u>very</u> high viscosity liquid is employed with a large diameter column.

Due to the high viscosity of the liquid, the generated small bubbles accumulate in the liquid increasing with the time of the gas injection as expected. Fig. 12 shows the increase of the concentration of the small bubbles with time at gas superficial velocity of 0.006 m/s. The population of the bubbles appears higher at the top section of the column. This is because a number of bubbles generated by the eruption of the large bubbles at the top are higher than those generated due to the effect of the gas injection points.

The volume fraction which occupied by the bubbles was divided by the total tested volume at the bottom and the top of the column. The volume of the bubbles was determined by removing the image background using a photo of the bubble column in the absence of the bubbles as a thresholding, (Otsu, 1980). The only limitation of this method is that it shows the volume occupied by the small bubble slightly larger than the actual volume. This is because the overlap caused by the bubbles behind them which are positioned next to the pipe wall. The rate of the overlap increases with increasing the population of the small bubbles. Table 1 shows the percentage of the volume occupied by the small bubble at the same location as Fig. 12. The volume occupied by the small bubbles increased as expected with increasing the time of gas injection at a constant gas flow rate using 5 gas nozzles (Philip, 1990). Moreover, the volume occupied by the small bubbles at the top section of the column was seen larger than the bottom section. It increased from 12.3% after 10 min of gas injection to 24.7% after 60 min at the top section, whereas it increased from 4.3% to 13% at 10 and 60 min, respectively. This agrees with the visual observations in the images in Fig. 12.

The rate of the small bubbles' formation in this work showed different results compared with the work presented by Pandit (1987) due to the difference in viscosities of the liquids. The mechanisms of the large bubble eruption in such high viscosity liquid showed a different behaviour compared with the method described by Pandit (1987). Fig. 5 illustrates the mechanisms of the bubble eruption in 330 Pa.s viscosity oil.

The liquid film above the bubble becomes thinner and rupture at the higher point when the pressure inside the bubble is higher than the atmospheric pressure due to the surface tension. The diameter of the hole created from the ruptured film remains smaller than the diameter of the ruptured bubbles. The ruptured film then collapses and fall inside the bubble trapping air as temporary bubbles which break down to small bubbles due to the shearing by the liquid motion. The rim of the hole of the ruptured bubbles seen as the same thickness as the ruptured film unlike the 1.0 Pa.s glycerol which employed in work by Pandit (1987). Therefore, comparing the rate of increasing the small bubble concentration in this work with (Pandit *et al.*, 1987) is not applicable.

3.4. Dimensions of the small bubbles

The diameter of the bubbles and the effect of the time of gas injection, in high viscosity liquids, was determined at a constant gas flow

rate. The same procedure in Section 3.3 was applied for the data acquisition. ImageJ software was used to scale and determine the bubbles diameters in both locations (top and bottom of the column). The bubble diameters shown in Table 2 are an average of 95 and 57 bubbles at the top and the bottom of the column respectively. This table can also be compared to the images in Fig. 12, which displays the size of the bubbles. In general, the average diameter of the bubbles changed in both locations to become approximately equal after one hour of gas injection. First, at the top section of the column, it increased slightly by 0.07 mm after 60 min of gas injection. While it decreased significantly by 0.353 mm at the bottom of the column to become almost equal to the diameters from the top section. As it has been explained in the previous section, the mechanism of generating the bubbles controls the size and the shape of the bubbles. The small bubbles, which are created from the collapsed film from the large bubbles rupture at the top section, are relatively smaller (0.68 mm average diameter) and more structured.

On the other hand, the bubbles produced at the bottom, due to the gas injection effect, are larger (1.1 mm average diameter) and variable in size, but they become homogenous by time due to the continuous mixing. After 60 min of gas injection, the average diameter in both locations becomes almost equal due to the mixing of the bubble inside the column. Therefore, at 0.006 m/s gas superficial velocity, the small bubbles, held up inside the column, become homogenous by 60 min time. This amount of time changes proportionally when changing the gas flow rate.

After 10 min in the top section, the diameters of the bubbles were about 5.8 to 0.2 mm. Then, after one hour, they became about 4.6 and 0.1 mm. The same scenario occurred at the bottom of the column; the diameter of the bubbles varied from about 4.6 to 0.3 mm and after one hour became about 1.49 and 0.17 mm. This variation is due to the effect of the mixing time. Although the number of the bubbles increases with time, the more mixing time between the bubbles leads to a decreasing in the variation of the size (i.e. making the distribution of the bubbles approximately uniform in size). In addition, the difference between the top and the bottom section in term of the bubble size is due to the nature of the mixing between both fluids in these areas as the bubbles creation mechanism in these areas are different, as discussed earlier. This can be seen in Fig. 13 which shows the Probability Density Function profile for the small bubbles diameter. The PDF was determined using the histogram method. It shows the variation in the values of bubbles diameter in the tested section. At the top section, bubbles with diameter of about 0.5 mm appears to dominate the structure. At the same time, the frequency of the dominated bubbles decreases after 60 min of gas injection. The bottom section showed different behaviour by displaying lower frequencies and wider range of bubble diameters. Besides, injecting gas for 60 min led to increase the frequency of bubbles of about 0.6 mm diameter. In result, both locations appear with approximately equal values of PDF/frequency for bubbles of 0.5-0.6 mm diameter. This might be due to the mixing between both sections or/and the coalescence and the breakup of the bubbles.

4. Conclusions

The dynamics of small bubbles created from the interaction of air flowing in 330 Pa.s Silicone oil and 290 mm diameter column as well as the contribution of the small bubbles in the overall void fraction in the column were investigated. ECT was employed for the overall gas holdup measurements. A high-resolution camera was used to obtain videos and photos of the small bubbles through the transparent wall of the columns. The observation of the small bubbles was achieved at two positions: first, at the top section of the column (at the top surface of the liquid) and, second, at about 0.6 m from the gas injection points at the bottom of the column. The main conclusions of the experiments carried out can be summarised as follows:

Table 1
The volume fraction of the small bubbles during the creation stage at the top and bottom section of the column at a gas superficial velocity of 0.006 m/s.

Bubbles volume fraction (%)		
Gas injection time	10 min	60 min
Top	12.358	24.278
Bottom	4.374	13.016

Table 2

The diameter of the small bubbles at the top and the bottom of the bubble column at two different times of gas injection at a constant gas superficial velocity of 0.006 m/s using 5 gas nozzles. Standard errors are calculated from the standard deviation and the square root of the number of the selected bubbles. The shaded cells are averaged values.

| | Bubbles Diameter (mm) | | | | | | | |
	10 min gas injection				60 min gas injection			
Top-column	Min.	0.2	Average	0.68	Min.	0.14	Average	0.75
	Max.	5.8	St. Error	0.06	Max.	4.6	St. Error	0.062
Bottom-column	Min.	0.3	Average	1.1	Min.	0.17	Average	0.747
	Max.	4.6	St. Error	0.1	Max.	1.9	St. Error	0.05

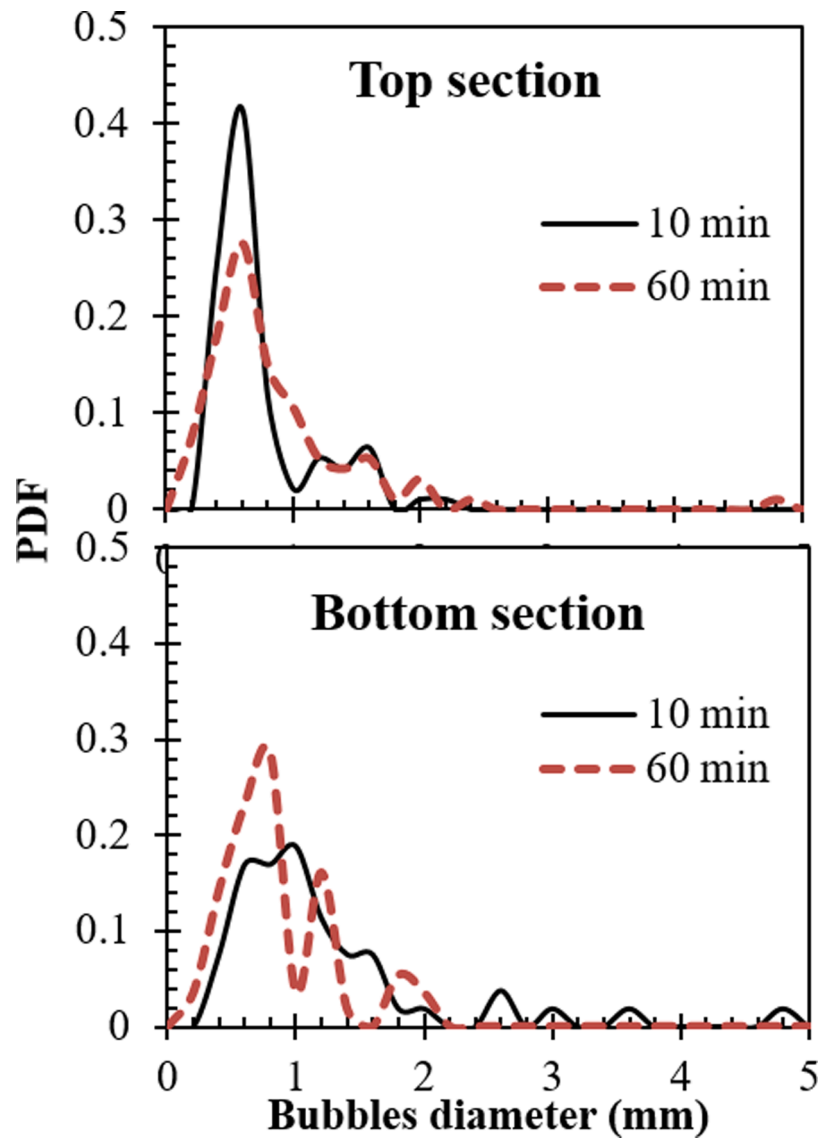Min.: Minimum; Max.: Maximum; St. Error: Standard Error

Figure 13. The Probability Density Function profile for the small bubbles diameter created by injecting gas for 60 min using 5 gas nozzles at constant superficial velocity (0.006 m/s) at two different locations in the column. The values in this figure correspond to the photos in Fig. 12.

1 Small bubbles in high viscosity liquids are generated from: bubble eruption at the top surface, gas injection points at the bottom of the column, coalescences between the large bubbles, and finally the churn regions in the column.

   a In bubble eruption, the rate of small bubbles generation increases with increasing the large bubbles frequency as well as the surface area of the liquid film created from the bubbles eruption.

   b At gas injection points, the bubbles are created from the rapid break up or coalescence of the large bubbles at the nozzles. The

large drag forces increase the possibility of the coalescence at the gas inlet points.

   c During the coalescence of the large bubble, small bubbles produce mainly due to the entrainment of two large bubbles of different rising velocity.

   d At churn areas in transition to churn flow regime, high frequency, and unstable direction of the motion of the liquid bridge, in addition to the high interaction between both fluids and the

drainage of the liquid film, all these factors control the rate of the small bubble generation.

2 The size, the shape and the population of the small bubbles are mainly controlled by the location of the bubble generation and the flow regime. The concentration of the bubbles is seen to be affected by gas flow rate, time of gas injection, number and location of the gas nozzles, and finally the location of the bubble generation.

3 The average diameter of the small bubbles at the top section appeared smaller than the average diameter at the bottom of the column at the start of gas injection. The average diameter became approximately equal (0.75 mm) in both sections after 60 min of gas injection and mixing.

4 Small bubbles volume fraction increased by approximately 24% and 13% at the top and the bottom sections respectively after 60 min of gas injection.

5 The contribution of the small bubbles to the total gas holdup depends on gas flowrate as well as the time of gas injection. Small bubbles seen to contribute by 8%, 6.6%, and 30% for bubbly, slug, and transition to churn flow regimes respectively after 6 h of gas injection.

Dedication

This work is dedicated to the memory of Professor Barry J Azzopardi a supervisor, colleague and good friend who passed away before publishing this work. The new findings reported in this work could not have been achieved without his knowledge, guidance and support.

CRediT authorship contribution statement

Shara K. Mohammed: Conceptualization, Methodology, Funding acquisition, Software, Formal analysis, Writing – original draft, Visualization. **Abbas H. Hasan:** Software, Validation, Writing – review & editing, Supervision. **Georgios Dimitrakis:** Resources, Writing – review & editing, Supervision. **Barry J. Azzopardi:** Conceptualization, Validation, Resources, Supervision.

Declaration of Competing Interest

The authors declare that they have no known competing financial interests or personal relationships that could have appeared to influence the work reported in this paper.

Acknowledgment

References

Abdulkareem, L.A., 2011. Tomographic investigation of gas-oil flow in inclined risers. University of Nottingham.

Aoyama, S., et al., 2016. Shapes of ellipsoidal bubbles in infinite stagnant liquids. Int. J. Multiph. Flow 79, 23–30. https://doi.org/10.1016/j.ijmultiphaseflow.2015.10.003.

Azzopardi, B.J., et al., 2010. Comparison between electrical capacitance tomography and wire mesh sensor output for air/silicone oil flow in a vertical pipe. Ind. Eng. Chem. Res. 49 (18), 8805–8811.

Azzopardi, B.J., Pioli, L., Abdulkareem, L.A., 2014. The properties of large bubbles rising in very viscous liquids in vertical columns. Int. J. Multiph. Flow 67, 160–173. https://doi.org/10.1016/j.ijmultiphaseflow.2014.08.013.

Azzopardi, B.J., Zaidi, S.H., 2000. Determination of entrained fraction in vertical annular gas/liquid flow. J. Fluids Eng. Trans. ASME 122 (1), 146–150. https://doi.org/10.1115/1.483236.

Bertola, V., 2003. Modelling and experimentation in two-phase flow. Springer Verlag.

Bhaga, D., Weber, M.E., 1981. Bubbles in viscous liquids: Shapes, wakes and velocities. J. Fluid Mech. 105 (1981), 61–85. https://doi.org/10.1017/S002211208100311X.

Bird, J.C., et al., 2010. Daughter bubble cascades produced by folding of ruptured thin films. Nature 465 (7299), 759–762. https://doi.org/10.1038/nature09069.

Bordel, S., Mato, R., Villaverde, S., 2006. Modeling of the evolution with length of bubble size distributions in bubble columns. Chem. Eng. Sci. 61 (11), 3663–3673. https://doi.org/10.1016/j.ces.2005.12.035.

Bröder, D., Sommerfeld, M., 2007. Planar shadow image velocimetry for the analysis of the hydrodynamics in bubbly flows. Meas. Sci. Technol. 18 (8), 2513–2528. https://doi.org/10.1088/0957-0233/18/8/028.

Colella, D., et al., 1999. A study on coalescence and breakage mechanisms in three different bubble columns. Chem. Eng. Sci. 54 (21), 4767–4777. https://doi.org/10.1016/S0009-2509(99)00193-1.

Costigan, G., Whalley, P.B., 1997. Slug flow regime identification from dynamic void fraction measurements in vertical air-water flows. Int. J. Multiph. Flow 23 (2), 263–282.

Ding, P., Bakalis, S., Zhang, Z., 2019. Foamability in high viscous non-Newtonian aqueous two-phase systems composed of surfactant and polymer. Colloids Surf. A Physicochem. Eng. Asp. https://doi.org/10.1016/j.colsurfa.2019.123817, 582 (August).

F. Kastánek et al. (1993) Chemical reactors for gas-liquid systems. Academia. Available at: https://scholar.google.com/scholar?hl=en&as_sdt=0%2C5&q=KASTÁNEK%2C+F.%2C+ZAHRADNÍK%2C+J.%2C+KRATOCHVÍL%2C+J.+%26+CERMÁK%2C+J.+1993.+Chemical+reactors+for+gas-liquid+systems.&btnG= (Accessed: 29 March 2021).

Fraser, R.P., Dombrowski, N., Routley, J.H., 1963. The atomization of a liquid sheet by an impinging air stream. Chem. Eng. Sci. 18 (6), 339–353. https://doi.org/10.1016/0009-2509(63)80027-5.

Hasan, A.H., et al., 2019. Gas rising through a large diameter column of very viscous liquid: flow patterns and their dynamic characteristics. Int. J. Multiph. Flow 116, 1–14.

Jamshidi, N., Mostoufi, N., 2017. Measurement of bubble size distribution in activated sludge bubble column bioreactor. Biochem. Eng. J. 125, 212–220. https://doi.org/10.1016/j.bej.2017.06.010.

de Jesus, S.S., Moreira Neto, J., Maciel Filho, R., 2017. Hydrodynamics and mass transfer in bubble column, conventional airlift, stirred airlift and stirred tank bioreactors, using viscous fluid: a comparative study. Biochem. Eng. J. 118, 70–81. https://doi.org/10.1016/j.bej.2016.11.019.

Kawalec-Pietrenko, B.T., 1992. Time-dependent gas hold-up and bubble size distributions in a gas-highly viscous liquid-solid system. Chem. Eng. J.

Kováts, P., Thévenin, D., Zähringer, K., 2020. Influence of viscosity and surface tension on bubble dynamics and mass transfer in a model bubble column. Int. J. Multiph. Flow 123. https://doi.org/10.1016/j.ijmultiphaseflow.2019.103174.

Kuncová, G., Zahradník, J., 1995. Gas holdup and bubble frequency in a bubble column reactor containing viscous saccharose solutions. Chem. Eng. Process. Process Intensif. 34 (1), 25–34.

Lage, P.L.C., Espósito, R.O., 1999. Experimental determination of bubble size distributions in bubble columns: Prediction of mean bubble diameter and gas hold up. In: Powder Technol. Elsevier Science S.A, pp. 142–150. https://doi.org/10.1016/S0032-5910(98)00165-X.

Lau, Y.M., et al., 2013. Experimental study of the bubble size distribution in a pseudo-2D bubble column. Chem. Eng. Sci. 98, 203–211. https://doi.org/10.1016/j.ces.2013.05.024.

Liu, Z., et al., 2020. Hydrodynamics of gas phase in a shallow bubble column from in-line photography. Chem. Eng. Sci. 221, 115703 https://doi.org/10.1016/j.ces.2020.115703.

Lubbert, A. et al. (1988) 'Fluid dynamics in airlift loop bioreactors as measured during real cultivation processes', in Proceedings of the BHRA 2nd International Conference on Bioreactor Fluid Dynamics. Oxford: R King (Ed) Elsevier Applied Science, pp. 379–393. Available at: https://scholar.google.com/scholar?hl=en&as_sdt=0%2C5&q=Fluid+dynamics+in+airlift+loop+bioreactors+as+measured+during+real+cultivation+processes%2C+paper+H1.&btnG= (Accessed: 29 March 2021).

Lucas, D., Ziegenhein, T., 2019. Influence of the bubble size distribution on the bubble column flow regime. Int. J. Multiph. Flow 120, 103092. https://doi.org/10.1016/j.ijmultiphaseflow.2019.103092.

Majumder, S.K., Kundu, G., Mukherjee, D., 2006. Bubble size distribution and gas-liquid interfacial area in a modified downflow bubble column. Chem. Eng. J. 122 (1–2), 1–10. https://doi.org/10.1016/j.cej.2006.04.007.

Maldonado, M., et al., 2020. A new approach to measure gas holdup in industrial flotation machines. Part II: Effect of fluid properties. Miner. Eng. 148, 106177 https://doi.org/10.1016/j.mineng.2019.106177.

Mandal, A., Kundu, G., Mukherjee, D., 2005. A comparative study of gas holdup, bubble size distribution and interfacial area in a downflow bubble column. Chem. Eng. Res. Des. 83 (4A), 423–428. https://doi.org/10.1205/cherd.04065.

Manga, M., Stone, H.A., 1994. Interactions between bubbles in magmas and lavas: effects of bubble deformation. J. Volcanol. Geotherm. Res. 63 (3–4), 267–279. https://doi.org/10.1016/0377-0273(94)90079-5.

Mena, P.C., et al., 2005. Using image analysis in the study of multiphase gas absorption. Chem. Eng. Sci. 60 (18), 5144–5150. https://doi.org/10.1016/j.ces.2005.04.049.

Mohammed, S.K., et al., 2018. Churn flow in high viscosity oils and large diameter columns. Int. J. Multiph. Flow 100, 16–29.

Mohammed, S.K., et al., 2019. Dynamics of flow transitions from bubbly to churn flow in high viscosity oils and large diameter columns. Int. J. Multiph. Flow 120, 103095.

Mohammed, S.K., et al., 2021. An experimental study on the effect of gas injection configuration on flow characteristics in high viscosity oil columns. Can. J. Chem. Eng. https://doi.org/10.1002/CJCE.24312.

Montante, G., Horn, D., Paglianti, A., 2008. Gas-liquid flow and bubble size distribution in stirred tanks. Chem. Eng. Sci. 63 (8), 2107–2118. https://doi.org/10.1016/j.ces.2008.01.005.

Otake, T., et al., 1977. Coalescence and breakup of bubbles in liquids. Chem. Eng. Sci. 32 (4), 377–383. https://doi.org/10.1016/0009-2509(77)85004-5.

Otsu, N., 1980. An Automatic Threshold Selrction Method Based on Discriminant and Least Squares Criteria. IEICEJ Trans. 69–500 (1), 349–356. Available at: https://ci. nii.ac.jp/naid/10015041440/ (Accessed: 19 March 2021).

Pandit, A.B., et al., 1987. The generation of small bubbles in liquids. In: International Chemical Reaction Engineering Conference, pp. 72–82.

Philip, J., et al., 1990. Gas hold-up and liquid circulation in internal loop reactors containing highly viscous Newtonian and non-Newtonian liquids. Chem. Eng. Sci. 45 (3), 651–664.

Pioli, L., et al., 2012. Experimental constraints on the outgassing dynamics of basaltic magmas. J. Geophys. Res. Solid Earth 117 (B3).

Pradeep, C., et al., 2014. Electrical capacitance tomography (ECT) and gamma radiation meter for comparison with and validation and tuning of computational fluid dynamics (CFD) modeling of multiphase flow. Meas. Sci. Technol. 25 (7), 75404.

Schäfer, R., Merten, C., Eigenberger, G., 2002. Bubble size distributions in a bubble column reactor under industrial conditions. Exp. Therm. Fluid Sci. 26 (6–7), 595–604. https://doi.org/10.1016/S0894-1777(02)00189-9.

Schumpe, A., Deckwer, W.D., 1987. Viscous media in tower bioreactors: hydrodynamic characteristics and mass transfer properties. Bioprocess Eng. 2 (2), 79–94. https://doi.org/10.1007/BF00369528.

Seyfried, R., Freundt, A., 2000. Experiments on conduit flow and eruption behavior of basaltic volcanic eruptions. J. Geophys. Res. Solid Earth 105 (B10), 23727–23740. https://doi.org/10.1029/2000jb900096.

Shah, Y.T., et al., 1982. Design parameters estimations for bubble column reactors. AIChE J. 28 (3), 353–379. https://doi.org/10.1002/aic.690280302.

Wongsuchoto, P., Charinpanitkul, T., Pavasant, P., 2003. Bubble size distribution and gas-liquid mass transfer in airlift contactors. Chem. Eng. J. 92 (1–3), 81–90. https://doi.org/10.1016/S1385-8947(02)00122-5.